

## THE CORROSION EFFECT of CuO and ZnO FORMATIONS ON BRASS SURFACE

**ABDULCABBAR YAVUZ<sup>\*1a</sup>, NECİP FAZIL YILMAZ<sup>2,3b</sup>, MAHMUT FURKAN KALKAN<sup>2c</sup>**

<sup>1</sup>Department of Metallurgical and Materials Engineering, Engineering Faculty, Gaziantep University, Sehitkamil, 27310, Gaziantep, TURKEY.

<sup>2</sup>Department of Mechanical Engineering, Engineering Faculty, Gaziantep University, Sehitkamil, 27310, Gaziantep, TURKEY.

<sup>3</sup>Board of Trustees, Hasan Kalyoncu University, Gaziantep, 27410, Turkey

\*ayavuz@gantep.edu.tr

### Abstract

A bulk brass containing Cu-Zn was oxidized at high temperatures (from 200 °C to 700 °C). The samples were cold rolled to reduce their thickness and the annealing process was applied. The specimens were heated at different temperatures in a furnace for the same duration (45 minutes). This paper examines the corrosion behavior of brass having an oxide surface obtained by heat treatment. The corrosion rate experiments were conducted by linear sweep voltammetry using a potentiostat. The corrosion properties of the specimens were analyzed by scanning the electrodes in saline water including 3.5% NaCl at the scan rate of 2 mV s<sup>-1</sup>. The corrosion behavior of the electrodes was investigated by two subsequent cycles. The change of the heated brass surface occurring after the corrosions test was also investigated. While the corrosion rate of the non-annealed brass electrode was similar to that of annealed specimens for the first scan, the corrosion rate of heat-treated specimens was dramatically decreased for the second scan. Pitting corrosion of non-heated brass and passivation behavior of heated brass electrodes were observed. Therefore, heat-treatment of brass can cause higher corrosion resistivity of the brass surface.

**Keywords:** Copper Oxide, Brass Alloy, Corrosion, Heat Treatment

### 1. Introduction

Corrosion is an important factor affecting both quality and economy all over the world.

The decomposition of the material into atoms or increasing the oxidation state of metals/alloys as a result of chemical reactions

How to cite this article:

Yavuz, A., Yilmaz, N.F., Kalkan, M.F., The Corrosion Effect of CuO And ZnO Formations on Brass Surface, The International Journal of Materials and Engineering Technology, 2021, 4(2): 117-124.

ORCID ID:

<sup>a</sup>0000-0002-7216-0586, <sup>b</sup>0000-0002-0166-9799, <sup>c</sup>0000-0002-1903-5583

is called corrosion [1]. Corrosion is an oxidation process that occurs when metals/alloys react with an oxidant such as oxygen that can be accelerated with temperature [2]. Briefly, the corrosion of material occurs either by the transformation of the metal/alloy onto its surface with a higher oxidation state or ion into a solution (environment) [3,4]. The most common and known natural resistance of corrosion is the passive layer formation which is generally a required process to avoid further corrosion. Passive film is an ultra-thin film that acts as a barrier against any reaction that may occur on the surface of a metal and can be formed spontaneously [5]. However, any metal which cannot have a passivating layer could hamper rusting easily [6]. Metals and alloys are commonly used in the food industry as preserving cups, Therefore, the corrosion resistivity of these boxes should be increased. The widespread use of metals depends on their specific properties [7]. Metals and alloys are selected depending on their properties including mechanical, electrical, thermal conductivity properties [8]. Additionally, corrosion resistance is an important parameter for materials selection [9]. More than hundreds of copper alloys can be used in various applications and some of them can be coated or copper can be alloyed to avoid corrosion [10]. Two of the most common alloys are bronze and brass. Brass has a yellowish color depending on the zinc and copper ratio [11]. Due to its flexibility and corrosion properties, brass is widely used especially in the marine field. Due to its use in the sea, brass is in constant danger of being sensitized to corrosion. Corrosion that occurs in the saltwater environment occurs faster than in the air environment [12,13]. Chloride ions can cause a serious risk of pitting corrosion, especially in materials that come into contact with saltwater [14].

A passive layer of copper oxide (CuO) could occur on the surface of copper alloys. These passive layers can protect the copper alloys from the corrosive media [15]. Also, some

studies have been concerned about CuO film applications on different material surfaces. The coating of the CuO film on stainless steel mesh improves the electrochemical performance of flexible stainless steel mesh [16]. Yetim et al. [17] observed that CuO nanoflowers can be used in energy materials. Koç [18] produced CuO-doped carbon photodiode specimen. The sample has a high potential for use as a substitute for graphene-based photodiode detectors. The main reason for zinc in brass is to increase its hardness, wear-resistance, and strength. According to investigations, the introduction of ZnO additions in electrical materials generates an increase in photodiode characteristics [19-21]. However, due to the inclusion of ZnO in the passive layer, brass could show lower pitting resistance than copper. Another important type of corrosion that occurs in brass is dezincification [22,23]. This is the result of selective corrosion of zinc, which is less noble than copper. As the zinc is exited from the brass lattice structure, voids are created and a porous Cu-structure remains. As a result, zinc can be removed from the brass faster than copper and leaves a porous, copper-rich and easily degradable metal on alloy surfaces [24]. This dezincification happens on all brass types, but some of them can have higher kinetics and some of them can take a long duration [25]. It is known that the mechanical properties of copper alloys such as brass can be improved by heat treatment [26]. The annealing process can increase the hardness and toughness of such materials [27-29]. In this study, the effect of the heat treatment process on the corrosion properties of brass samples was investigated. The corrosion resistivity of the bulk brass was not examined. The electrochemical behavior of the brass surface in the NaCl solution was elucidated. The electrochemical test was applied to the samples in the sodium chloride environment. Pitting corrosion and passivation behavior of non-heated and heated samples were examined. Linear sweep voltammetry was applied twice to non-

annealed and annealed brass samples (heated at 200, 300, 400, 500 and 700 °C for 45 minutes).

## 2. Materials and Methods

0.2 mm thick brass electrode consisting of 60% copper and 40% zinc mixture was prepared by the rolling process. The cross-section of brass electrodes was respectively ground mechanically with 300, 600 and 1000 grit SiC sandpapers. The brass electrodes were cut 1 cm in width. They were washed with water and dried with hot air. The heat treatment process was applied to the brass electrodes in a muffle furnace. Different temperatures were used to compare with the original electrode. The set temperature was 200, 300, 400, 500 and 700 °C. The duration of all brass heating was 45 minutes. Three samples were left in the furnace at each temperature to repeat the corrosion experiments. AMETEK VERSASTAT 3-200 potentiostat was used for corrosion studies and the cyclic polarization technique was applied at room temperature. The cycling electrolyte of 3.5% (by weight) NaCl in distilled water was prepared to be used in the experiments shown in this study. 3.5% (by weight) NaCl solution can corrode a metal similar to seawater. A silver/silver chloride electrode (Ag/AgCl) was used to measure the potential of the electrode. Before the corrosion tests, all samples were cleaned with distilled water. Corrosion test scan was started at a potential which was -0.3 V less than open circuit potential. The vertex potential of the electrode cycling in NaCl solution was +0.8 V. All potential presented in this research was given against silver/silver chloride reference electrode having saturated potassium chloride. Two cycles were applied to all measurements. The final potential of cycling was again the potential which was the value 0.3 V less than open circuit potential (from the left-hand side of open circuit potential). The scan rate for all brass electrodes was 2 mV/s because a higher scan rate is not useful to indicate the corrosion rate.

## 3. Results and Discussion

Cold rolled brass electrode (60% Cu with 40% Zn) was heated in a muffle furnace. The furnace was preheated to 200, 300, 400, 500 and 700 °C. Brass electrodes were oxidized thermally in the furnace for 45 minutes. As it was indicated that three samples were annealed in the furnace without opening its door. The electrodes were directly immersed in NaCl solution as a working electrode. Linear sweep voltammetry is normally used for the corrosion response of electrodes in the NaCl solution. However, in this study, a cyclic polarization was applied to observe the pitting behavior of the annealed brass. The Tafel plot obtained as a result of the cyclic polarization test of oxidized brass applied in NaCl corrosive environment is given in Figure 1a. During the cyclic polarization test, two consecutive cycles were performed for each sample. Figure 1(a) and Figure 1(b) show the Tafel plot of the first oxidation from a negative to a positive direction. Figure 1(b) is the magnified version of Figure 1(a) in order to explore the  $E_{\text{corr}}$  and  $I_{\text{corr}}$  values. Corrosion current density ( $I_{\text{corr}}$ ) is obtained by the intersection of the anodic and cathodic branches of the polarization curves on the Tafel plot of the samples tested. In the same graph, the point obtained by the extension of the anodic and cathodic branches through voltage axes is called the corrosion potential ( $E_{\text{corr}}$ ). The  $E_{\text{corr}}$  and  $I_{\text{corr}}$  values obtained from Figure 1 are shown in Table 1.

While the corrosion potential of non-annealed brass was -0.18 V, it was generally decreased (going to more negative potential) upon increasing annealing temperature as observed in Figure 1. The corrosion potential of the electrode heated at 200, 300, 400, 500 °C was -0.196, -0.225, -0.235 and -0.318 V, respectively. The only exception which did not follow the decreasing trend was the electrode heated at 700 °C. The corrosion potential of the brass heated at 700 °C was -0.240 V. This could occur probably due to the oxidation state of the zinc and copper in the brass [30] for example copper becomes  $\text{Cu}_2\text{O}$

and CuO at 300 °C and 600 °C [31]. The corrosion current value of the non-heated brass was  $10^{-5.25}$  A cm<sup>-2</sup> ( $5.6 \mu\text{A cm}^{-2}$ ). The corrosion current for the electrodes annealed at 200, 300, 400, 500 and 700 °C was  $10^{-5.70}$ ,  $10^{-6.10}$ ,  $10^{-5.20}$ ,  $10^{-5.60}$  and  $10^{-5.83}$  A cm<sup>-2</sup>, respectively as presented in Table 1. They corresponded to  $2.0 \mu\text{A cm}^{-2}$ ,  $0.8 \mu\text{A cm}^{-2}$ ,  $6.3 \mu\text{A cm}^{-2}$ ,  $2.5 \mu\text{A cm}^{-2}$  and  $1.5 \mu\text{A cm}^{-2}$ . These results show that corrosion current which is directly proportional to corrosion rate did not change significantly because the corrosion current of the annealed brasses was generally close to that of non-annealed brass

( $5.6 \mu\text{A cm}^{-2}$ ). The corrosion rate of heated brass at 300 °C ( $0.8 \mu\text{A cm}^{-2}$ ) was seven times lower than that of unheated brass ( $5.6 \mu\text{A cm}^{-2}$ ). Therefore, corrosion resistance of annealed brass at 300 °C was found higher than the non-heat treated electrode surface. The corrosion resistance that occurs with the application of heat treatment at 300 °C is thought to be caused by the copper oxide formed on the surface. However, other temperatures can not significantly increase the corrosion resistivity of the brass electrode.

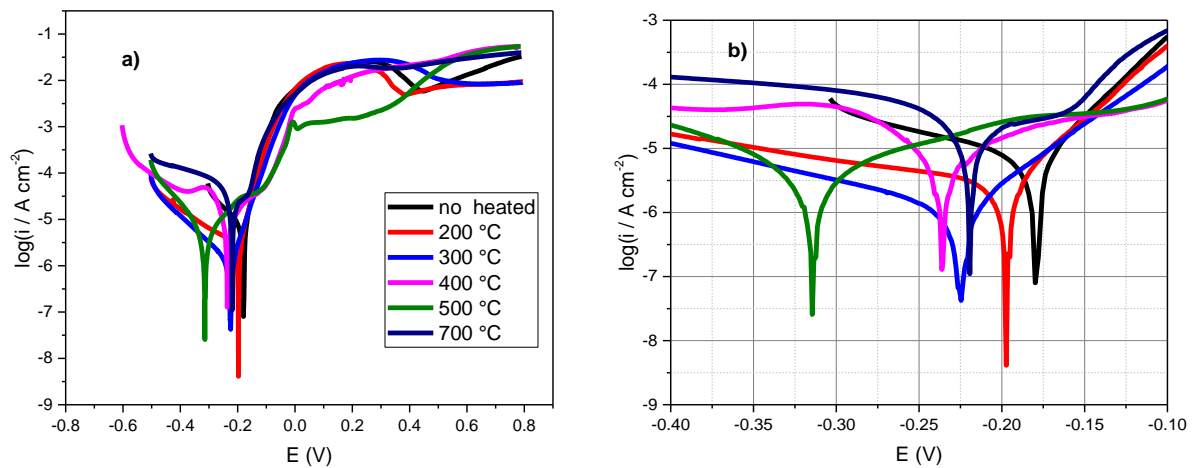


**Figure 1.** a) First cycles of Tafel polarization curves for heated at different temperatures, b) Magnification of panel to illustrate Tafel polarization curves

**Table 1.**  $E_{\text{corr}}$  and  $I_{\text{corr}}$  data measured from Tafel plot of the first loop

| Sample  | $E_{\text{corr}}$ (V) | $I_{\text{corr}}$ (A cm <sup>-2</sup> ) |
|---------|-----------------------|---|
| No heat | -0.180                | $10^{-5.25}$                            |
| 200 °C  | -0.196                | $10^{-5.70}$                            |
| 300 °C  | -0.225                | $10^{-6.10}$                            |
| 400 °C  | -0.235                | $10^{-5.20}$                            |
| 500 °C  | -0.318                | $10^{-5.60}$                            |
| 700 °C  | -0.240                | $10^{-4.83}$                            |

When the Tafel curve of the first cycle was examined, it was observed that as the temperature applied to the electrodes in the furnace increased, the corrosion resistance did not change significantly. However, the brass electrode exposed to a temperature of 700 °C gave a curve whose corrosion potential was close to the corrosion potential

of the electrode exposed to a temperature of 300 and 400 °C. It was estimated that this may occur due to the change in the structure of the material heated at a different temperature. The heated electrodes were scanned between a negative potential up to 0.8 V and their Tafel plots were presented in Figure 1. The same electrodes were not taken

from the NaCl solution and they were again polarized between the same potential windows. The second sweeps of non-heated and heated specimens in NaCl solution are presented in Figure 2a. The closer look of the linear sweep voltammetry given in Figure 2(a) is shown in Figure 2(b). Corrosion currents and potentials of the electrodes are tabulated in Table 2.

The corrosion potential of the non-heated electrode cycled in NaCl solution for the second time was -0.083 V. The corrosion potential of the electrodes decreased significantly. It can be seen in Figure 2 and Table 2 that the corrosion potential of the heated electrode in the NaCl bath for the second sweeping was not affected by the annealing temperature. The corrosion potential of brass electrodes heated at 200, 300, 400, 500 °C was around -0.2 V. The second corrosion current of the non-annealed electrode was  $10^{-3.36}$  A cm<sup>-2</sup> (436 μA cm<sup>-2</sup>). It was shown above that the first corrosion current of the non-treated electrode was 5.6 μA cm<sup>-2</sup>. Therefore, the corrosion rate of the

non-annealed brass electrode increased 78 times from 5.6 μA cm<sup>-2</sup> to 436 μA cm<sup>-2</sup>. This means that an electrode polarized in the NaCl pool can be 78 times more readily oxidized (corroded) in the second polarization. This behavior has been indicated for pitting corrosion of metals and alloys in the literature [31]. The corrosion current for the brasses heated at 200, 300, 400, 500 and 700 °C was  $10^{-4.83}$ ,  $10^{-4.90}$ ,  $10^{-4.88}$ ,  $10^{-4.45}$  and  $10^{-4.32}$  A cm<sup>-2</sup>, respectively as given in Table 2. The corrosion current for these electrodes were respectively 14.8 μA cm<sup>-2</sup>, 12.6 μA cm<sup>-2</sup>, 13.2 μA cm<sup>-2</sup>, 35.5 μA cm<sup>-2</sup>, and 47.9 μA cm<sup>-2</sup>. The corrosion rate of the electrodes swept for the second time was similar to that for the first time. Therefore, it could be concluded that the heated electrodes were passivated after the first polarization. The effect of temperature was not observed for the passivation of the electrodes. Heating at any temperature from 200 °C to 300 °C could create a passive layer on the bulk brass surface.

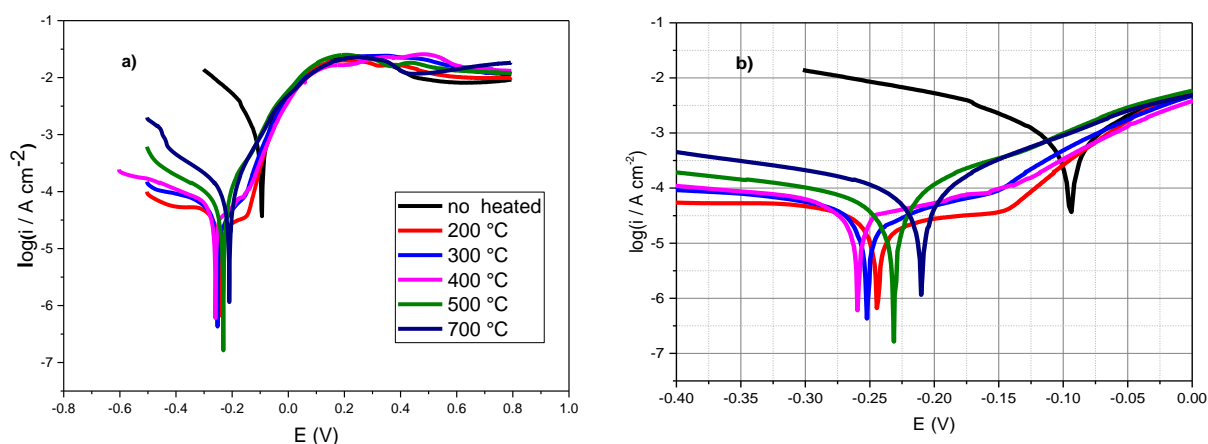


**Figure 2.** a) Second cycles of Tafel polarization curves for heated at different temperatures, b) Magnification of panel to illustrate Tafel polarization curves

Unlike the first cycle, heating the electrodes directly affected the corrosion rates in the second cycle. It was observed that heating the electrode using a heat treatment furnace created a significant difference in corrosion resistance during the second cycle. The corrosion current density of the non-heated

electrode was 35 times higher than that of heated at 300 °C brass. This shows that pitting corrosion is not significant in the heated brass and the passive layer of heated brass at 300 °C was found stronger than the original electrode surface. Copper oxide, which provides the passive layer formed by

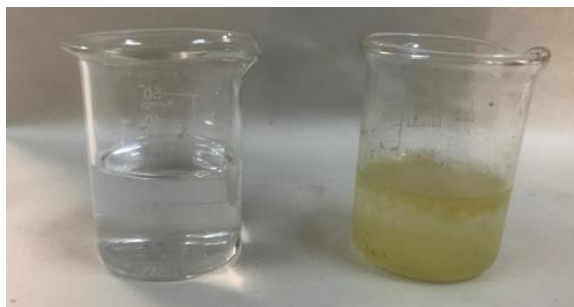
collecting brass electrodes, is thought to be more effective at annealing temperatures of 300 °C, 400 °C and 200 °C. Although the heating of the electrodes did not have a significant difference in the first corrosion cycled in the %3.5 NaCl bath, it was observed that it affected the formation of significant corrosion resistance in the next cycle due to the presence of a passive layer.

Figure 2 (a) shows the typical photo of the NaCl solution before and after linear sweep voltammetry of a heated brass. While the color of the NaCl solution was transparent, it

was turned to yellow color after polarization presented in Figure 2. Figure 3(b) shows the photo of the heated brass electrode before and after being tested in NaCl electrolyte. The color change in the part immersed in liquid can be given as an example of dezincification. It can be deduced from its red color which is well known for copper. It was seen that the zinc atoms left the surface when it was in the %3.5 NaCl environment and brass had a copper-rich region on the electrode area.

**Table 2.**  $E_{\text{corr}}$  and  $I_{\text{corr}}$  data measured from Tafel plot of the second loop

| Sample  | $E_{\text{corr}}$ | $I_{\text{corr}}$ |
|---------|-------------------|-------------------|
| No heat | -0.083            | $10^{-3.36}$      |
| 200 °C  | -0.242            | $10^{-4.83}$      |
| 300 °C  | -0.251            | $10^{-4.90}$      |
| 400 °C  | -0.267            | $10^{-4.88}$      |
| 500 °C  | -0.232            | $10^{-4.45}$      |
| 700 °C  | -0.210            | $10^{-4.32}$      |



(a)



(b)

**Figure 3.** a) Photos of 3.5% NaCl solution before polarization (left side) and after polarization (right side) of heated brass. b) Photos of heated bulk brass before polarization (left side) and after polarization (right side) in 3.5% NaCl solution.

#### 4. Conclusions

Cold rolled brass having 60% Cu with 40% Zn was annealed at 200, 300, 400, 500 and 700 °C in a furnace for 45 minutes. The resultant electrodes were transferred to NaCl electrolyte for corrosion test. The test was conducted by sweeping voltage from a negative potential to 0.8 V against silver/silver chloride electrode at the scan rate of 2 mV s<sup>-1</sup>. The Tafel plots of heated brass electrodes were obtained for two subsequent

scans. Corrosion current density of unheated samples for the first scan was not changed dramatically when the annealing temperature increased. However, the corrosion potential of the heated brass decreases with increasing the temperature up to 500 °C. The corrosion potential of the brass annealed at 700 °C was similar to that at 300 °C probably because of a different form of oxidation at high temperatures. The corrosion resistivity of the non-annealed and annealed brasses was

similar to each other for the first scan as the corrosion current values of them were close to each other. However, the corrosion current of annealed samples was significantly decreased for the second scan. Therefore, the corrosion rate of the brass could be decreased significantly (around 50 times) by annealing. Additionally, the corrosion potential of heated brasses scanned for the second time in NaCl solution was similar to each other and did not depend on temperature. This occurred because unheated brass could have pitting corrosion and annealed brass can have a passive layer in NaCl solution. This situation was proved by the color change of the brasses and the electrolyte in which brasses were polarized.

### Acknowledgments

This work was supported by Gaziantep University Scientific Research Unit (MF.ALT.19.18). The authors would like to express their deepest appreciation to the organizing committee of TICMET20 in the selection of this study which was presented in the conference organized on 5-7 November, 2020 in Gaziantep University.

### References

1. Verma, C., Ebenso, E.E., Quraishi, M.A., Ionic liquids as green and sustainable corrosion inhibitors for metals and alloys: an overview. *J Mol Liq.* **2017**, 233:403–14.
2. Gülerüz, H., Çimenoglu, H., Effect of thermal oxidation on corrosion and corrosion–wear behaviour of a Ti–6Al–4V alloy. *Biomaterials.* **2004**, 25(16):3325–33.
3. Indra, A., Menezes, P.W., Zaharieva, I., Baktash, E., Pfrommer, J., Schwarze, M., et al., Active Mixed-Valent MnOx Water Oxidation Catalysts through Partial Oxidation (Corrosion) of Nanostructured MnO Particles. *Angew Chemie Int Ed.* **2013**, 52(50):13206–10.
4. Gu, B., Luo, J., Mao, X., Hydrogen-facilitated anodic dissolution-type stress corrosion cracking of pipeline steels in near-neutral pH solution. *Corrosion.* **1999**, 55(1):96–106.
5. A titanium-doped SiO<sub>x</sub> passivation layer for greatly enhanced performance of a hematite-based photoelectrochemical system. *Angew Chem, Int Ed [Internet].* **2016**, 55:9922.
6. Kihira, H., Ito, S., Murata, T., The behavior of phosphorous during passivation of weathering steel by protective patina formation. *Corros Sci.* **1990**, 31:383–8.
7. Baksan, B., Çelikyürek, İ., Kılıç, Y., Effect of secondary aging of EN AC 43200 Aluminum alloy to mechanical properties. *Int J Mater Eng Technol.* **2020**, 3(1):16–20.
8. Jin, K., Sales, B.C., Stocks, G.M., Samolyuk, G.D., Daene, M., Weber, W.J., et al., Tailoring the physical properties of Ni-based single-phase equiatomic alloys by modifying the chemical complexity. *Sci Rep.* **2016**, 6:20159.
9. Sandström, R., An approach to systematic materials selection. *Mater Des.* **1985**, 6(6):328–38.
10. Chen, S., Brown, L., Levendorf, M., Cai, W., Ju, S-Y., Edgeworth, J., et al., Oxidation resistance of graphene-coated Cu and Cu/Ni alloy. *ACS Nano.* **2011**, 5(2):1321–7.
11. Walter, B., Process for manufacturing brass and bronze alloys containing lead. *Google Patents; 1957.*
12. Ravichandran, R., Rajendran, N., Electrochemical behaviour of brass in artificial seawater: effect of organic inhibitors. *Appl Surf Sci.* **2005**, 241(3–4):449–58.
13. Santos, C.I.S., Mendonça, M.H., Fonseca, I.T.E., Corrosion of brass in natural and artificial seawater. *J Appl Electrochem.* **2006**, 36(12):1353–9.
14. Ezuber, H., El-Houd, A., El-Shawesh, F., A study on the corrosion behavior of aluminum alloys in seawater. *Mater Des.*

- 2008, 29(4):801–5.
15. Malav, J.K., Rathod, R.C., Tandon, V., Patil A.P., Enhancement of corrosion protection of low nickel austenitic stainless steel by electroactive polyimide-CuO composites coating in chloride environment. *Anti-Corrosion Methods Mater.* **2019**.
  16. Yavuz, A., Kaplan, K., Bedir, M., Copper oxide coated stainless steel mesh for flexible electrodes. *J Phys Chem Solids.* **2021**, 150:109824.
  17. Yetim, N.K., Aslan, N., Sarıoğlu, A., Sarı N., Koç, M.M., Structural, electrochemical and optical properties of hydrothermally synthesized transition metal oxide (Co<sub>3</sub>O<sub>4</sub>, NiO, CuO) nanoflowers. *J Mater Sci Mater Electron.* **2020**, 31(15):12238–48.
  18. Koc, M.M., Photoelectrical properties of solar sensitive CuO doped carbon photodiodes. *J Mol Struct.* **2020**, 1208:127872.
  19. Koç, M.M., Aslan, N., Erkovan, M., Aksakal, B., Uzun, O., Farooq, W.A., et al., Electrical characterization of solar sensitive zinc oxide doped-amorphous carbon photodiode. *Optik (Stuttg).* **2019**, 178:316–26.
  20. Karabulut, A., Dere, A., Al-Sehemi, A.G., Al-Ghamdi, A.A., Yakuphanoglu, F., Zinc oxide based 3-components semiconductor oxide photodiodes by dynamic spin coating method. *Mater Sci Semicond Process.* **2021**, 134:106034.
  21. Zhang, T-F., Wu, G-A., Wang, J-Z., Yu, Y-Q., Zhang, D-Y., Wang, D-D., et al., A sensitive ultraviolet light photodiode based on graphene-on-zinc oxide Schottky junction. *Nanophotonics.* **2017**, 6(5):1073–81.
  22. Polunin, A.V., Pchel'nikov, A.P., Losev, V.V., Marshakov, I.K., Electrochemical studies of the kinetics and mechanism of brass dezincification. *Electrochim Acta.* **1982**, 27(4):467–75.
  23. Sugawara, H., Ebiko, H., Dezincification of brass. *Corros Sci.* 1967;7(8):513–23.
  24. Karpagavalli, R., Balasubramaniam, R., Development of novel brasses to resist dezincification. *Corros Sci.* **2007**, 49(3):963–79.
  25. Rojas-Rodríguez, I., Lara-Guevara, A., Salazar-Sicacha, M., Mosquera-Mosquera, J.C., Robles-Agudo, M., Ramirez-Gutierrez, C., et al., The Influence of the Precipitation Heat Treatment Temperature on the Metallurgical, Microstructure, Thermal Properties, and Microhardness of an Alpha Brass. *Mater Sci Appl.* **2018**, 9(4):440–54.
  26. Tecer, M.M., Effects of various heat treatment procedures on the toughness of aisi 4140 low alloy steel. *Int J Mater Eng Technol.* 3(2):131–49.
  27. Loukus, A., Loukus, J., Heat Treatment Effects on the Mechanical Properties and Microstructure of Preform-Based Squeeze Cast Aluminum Metal Matrix Composites. *Int J Met.* **2011**, 5(1):57–65.
  28. Kim, H.S., Kim, W.Y., Song, K.H., Effect of post-heat-treatment in ECAP processed Cu–40% Zn brass. *J Alloys Compd.* **2012**, 536:S200–3.
  29. Kaur, M., Muthe, K.P., Despande, S.K., Choudhury, S., Singh, J.B., Verma, N., et al., Growth and branching of CuO nanowires by thermal oxidation of copper. *J Cryst Growth.* **2006**, 289(2):670–5.
  30. Balık, M., Bulut, V., Erdogan, I.Y., Optical, structural and phase transition properties of Cu<sub>2</sub>O, CuO and Cu<sub>2</sub>O/CuO: Their photoelectrochemical sensor applications. *Int J Hydrogen Energy.* **2019**, 44(34):18744–55.
  31. Büyüksağış, A., Kayalı, Y., Investigation of Corrosion Behaviours Hydroxyapatite (HAP) coated Ti6Al4V Implants by Using Electrochemical Deposition Method. *Afyon Kocatepe Üniversitesi Fen Ve Mühendislik Bilim Derg.* **2018**, 18(3):807–19.